The 5-HT$_3$AB Receptor Shows an A_3B_2 Stoichiometry at the Plasma Membrane

Timothy F. Miles,[†] Dennis A. Dougherty,[‡] and Henry A. Lester[†*]
[†]Division of Biology and Biological Engineering and [‡]Division of Chemistry and Chemical Engineering, California Institute of Technology, Pasadena, California

ABSTRACT The 5-HT$_3$AB receptor is the best-characterized heteropentameric 5-HT$_3$ receptor. Under conditions of heterologous expression, the 5-HT$_3$AB receptor shows a single functionally resolvable population, suggesting the presence of a unique subunit stoichiometry; however, conflicting previous reports have suggested two different possible stoichiometries. Here we isolate plasma membrane sheets containing assembled receptors from individual HEK293T cells. We then determine the stoichiometry of 5-HT$_3$AB receptors on the plasma membrane by fluorescence methods, employing meCFP- and meYFP-labeled A and B subunits. Over a wide range of cDNA transfection ratios, fluorescence intensity ratios are closest to values that correspond to a subunit ratio of A_3B_2. Förster resonance energy transfer (family FRET) efficiencies provide minor corrections (3–6%) to the subunit ratios and provide independent support for a predominantly A_3B_2 stoichiometry on the plasma membrane sheets. Twin FRET efficiencies support these data, also suggesting that the two B subunits are nonadjacent in most of the heteropentamers. The high-frequency variant *HTR3B* p.Y129S (c.386A>C, rs11767445), linked to psychiatric disease, also forms A_3B_2 receptors on the plasma membrane. The 5-HT$_3$B Y129S, subunit incorporates in a slightly (11–14%) more efficient manner than the common variant. In general, most of the subunits reside within the cell. In contrast to the findings for the plasma membrane, the relative abundances and FRET characteristics of intracellular subunits depend strongly on the transfection ratio. The straightforward and unambiguous combination of plasma membrane-sheet isolation, fluorescence intensity ratios, and FRET is a generally promising procedure for determining stoichiometry of proteins on the plasma membrane.

INTRODUCTION

Recognition of serotonin (5-HT) is accomplished by the various proteins (including enzymes, transporters, and receptors) that regulate its fundamental role in neurotransmission. Among the seven families of serotonin receptor, only one is an ion channel. The 5-HT$_3$ receptor, as a member of the Cys-loop superfamily of ligand-gated ion channels, is composed of five subunits that arrange symmetrically around a central pore (1,2). Found in both the peripheral and central nervous systems, 5-HT$_3$ receptors have been implicated in numerous salutary and pathological processes including emesis, nociception, cognition, and depression (3,4).

Once believed to consist of only one member (5-HT$_3$A), the known 5-HT$_3$ receptor family has recently been expanded by identification of four additional subunits (B–E) (4–6). Unlike 5-HT$_3$A, which is capable of forming functional homopentameric receptors, the B–E subunits convey function only in the presence of the A subunit as heteromers. The best studied of these, 5-HT$_3$AB, differs greatly from the homomeric receptor (7). For 5-HT, the AB receptor shows an increased EC_{50} and rate of desensitization coupled with decreased cooperativity, inward rectification, and calcium permeability (5,8–10). Major differences in pharmacological selectivity at allosteric sites have also been observed (7,11,12). Moreover, only the markedly higher conductance of the 5-HT$_3$AB receptor agrees with that observed in native tissue (13–16). Heteromeric receptors containing 5-HT$_3$C, D, or E subunits, on the other hand, are as yet functionally indistinguishable from the homomeric receptor (17,18).

As heteropentamers, functional 5-HT$_3$AB receptors may exhibit numerous potential subunit stoichiometries. Unlike other members of the Cys-loop superfamily, however, the 5-HT$_3$AB receptor shows a single functionally resolvable population in heterologous expression systems. In an early study aimed at determining the stoichiometry of this population, purified 5-HT$_3$AB receptors were antibody-labeled at epitope tags specific to the A and B subunits (19). AFM was then used to observe the angle between adjacent antibodies. For the 5-HT$_3$AB receptor, two inter-antibody angles were observed: one that is unique to the heteromer and one that is also seen in the homomer. Based on the pattern of these angles, the authors proposed that receptors are composed of two A subunits and three B subunits arranged B-B-A-B-A.

Because the orthosteric ligand-binding site of Cys-loop receptors spans the interface of two adjoining subunits, this finding suggested that the B subunit must successfully contribute to the gating of 5-HT$_3$AB receptors. Recent studies, however, have called this conclusion into question. While conversion of critical A subunit residues to the identity of that in the B subunit is strongly deleterious to orthosteric ligand binding, the corresponding mutations from B to A exhibit no effect (20). Further, introduction of double cysteine mutants (placed one per face on a potential binding site) in the A subunit displayed no response in

Submitted May 16, 2013, and accepted for publication July 11, 2013.

*Correspondence: lester@caltech.edu

Editor: Cynthia Czajkowski.

© 2013 by the Biophysical Society

0006-3495/13/08/0887/12 $2.00

http://dx.doi.org/10.1016/j.bpj.2013.07.015

either homo- or heteromeric receptors until exposed to a reducing agent. Finally, it was shown that cysteine labeling near the postulated AB orthosteric site hinders ligand binding only for A subunit residues (21). Together these findings suggested, contrary to the AFM data (19), the presence of at least one A-A subunit interface in the 5-HT_3AB receptor.

In this study, we have sought to resolve the stoichiometry of functional membrane 5-HT_3AB receptors using various fluorescence methods on isolated membrane sheets from whole cells expressing fluorescent protein fusions of the 5-HT_3A and B subunits.

MATERIALS AND METHODS

Materials

The pcDNA3.1(+) expression vector, and fetal bovine serum reagents, were purchased from Invitrogen (Carlsbad, CA). TransIT transfection reagent was purchased from Mirus (Madison, WI). Penicillin/streptomycin (100×) solution was purchased from Mediatech (Herndon, VA). Culture dishes (35 mm, with 14-mm, No. 0 thickness, glass coverslip microwells) were purchased from Mattek (Ashland, MA). Coverslips (25 mm, No. 1 thickness glass) were purchased from VWR (Radnor, PA). Other tissue-culture plasticware was purchased from Greiner Bio-One (Monroe, CA).

Molecular biology

Monomeric-enhanced (me) CFP and YFP were introduced in frame into the M3-M4 loops of the human 5HT3A and 5HT3B subunits, taking care to avoid known signaling and trafficking motifs. The forward primer

5′-AAG ACT GAT GAC TGC TCA GCC ATG GGA AAC CAC TGC AGC CAC ATG GGA GCT GGC GCC ATG GTG AGC AAG GGC GAG GAG-3′

and the reverse primer

5′-GGG AGG GCT ACA TCT GTC CCT CGG GCT CTT CTC GAA GTC CTG GGG TCC GGC GCC TGC CTT GTA CAG CTC GTC CAT GCC-3′

were used in PCR to add overlapping regions homologous to the M3-M4 region of h5-HT3A to meCFP and meYFP. The forward primer

5′- GCT AAG TCC ATC GTG TTG GTC AAA TTC CTC CAT GAT GAG CAG CGT GGT GCT GGC GCC ATG GTG AGC AAG GGC GAG GAG-3′

and the reverse primer

5′-GGT TCC TGG CTG GGC CAG GTG CTC TCC ATA CAG CGA GGA CTC TGT TAC GGC GCC TGC CTT GTA CAG CTC GTC CAT GCC-3′

were used in PCR to add overlapping regions homologous to the M3-M4 region of h5-HT3B to meCFP and meYFP. These products were then isolated and used as inserts in a second PCR reaction with the corresponding full-length subunit to generate the receptor subunit-fluorescent protein fusion constructs. The fluorescent protein insertion point for the A subunit is between Gly-421 and Gly-422. The insertion point for the B subunit is between Gly-333 and Gly-334. All constructs were verified by sequencing.

Cell culture and transfection

Human embryonic kidney (HEK) 293T cells, bearing T-antigen, were maintained on 100-mm culture plates at 37°C and 5% CO_2 in a humidified atmosphere. They were cultured in Dulbecco's modified Eagle's medium/nutrient mix F12 (1:1) with GlutaMAX I media (Invitrogen) containing 10% fetal calf serum and penicillin/streptomycin. Cells at 60–80% confluency within 35-mm dishes were transfected with a total of 2 μg of plasmid DNA using the TransIT transient transfection kit (Mirus). For FlexStation studies (Molecular Devices, Eugene, OR), cells were transfected and then plated in 96-well plates. Cells were incubated 1–2 days before assay. For whole-cell fluorescence studies, cells were plated in 35-mm glass-bottomed dishes and imaged one day after transfection. For membrane isolation studies, cells were prepared four days after transfection.

FlexStation analysis

The FlexStation (Molecular Devices) analysis technique uses fluorescent voltage-sensitive dyes to detect changes in the membrane potential. It has been used to examine various ion channels, including those of the 5-HT_3 receptors (22). In brief, fluorescent membrane potential dye (Molecular Devices) was diluted in the Flex buffer (10 mM HEPES, 115 mM NaCl, 1 mM KCl, 1 mM $CaCl_2$, 1 mM $MgCl_2$, and 10 mM glucose, pH 7.4) and added to transfected cells grown on a 96-well plate. The cells were incubated at room temperature for 30 min and then fluorescence was measured in a FlexStation (Molecular Devices) at 2-s intervals for 200 s. Serotonin (5-HT) was added to each well after 20 s. The percentage change in fluorescence was calculated as

$$\frac{(F - F_{\min})}{F_{\max}},$$

where F is peak fluorescence for the current agonist dose, $F_{\max}$ is peak fluorescence at saturating agonist and $F_{\min}$ is baseline fluorescence at 20 s.

To determine EC_{50} values, concentration-response data were fitted to the four-parameter logistic equation,

$$I = \frac{I_{\max}}{\left[1 + \left(\frac{EC_{50}}{[A]}\right) n_H\right]},$$

where $I_{\max}$ is the maximal response plateau, [A] is the log concentration of agonist, and n_H is the Hill coefficient, using KaleidaGraph v3.6 software (Synergy Software, Reading, PA).

Membrane isolation

When one performs ensemble measurements of integral membrane proteins on the plasma membrane, it is important to restrict the pool of observed subunits to only those that reside on the plasma membrane. To isolate this restricted population, membrane was mechanically removed from the rest of the cell as described previously in Perez et al. (23).

This is achieved by bathing HEK293T cells 72–96 h posttransfection in deionized water to induce swelling. After 1 min, a No. 1 coverslip, sterilized by sequential 20-min 6-M KOH and acetone baths with sonication and stored in 20-μm filtered deionized water, was placed on top of the cells. Pressure was applied to the coverslip with a pipette tip for 3 min ensuring contact with the cell membrane. The coverslip was then removed, bringing adhered membrane with it, and thoroughly rinsed with phosphate-buffered saline (PBS) to remove remaining intracellular contents. To ensure complete intracellular removal, all samples subjected to this preparation were transfected with DsRed2-ER, which labels endoplasmic reticulum (ER).

The membrane-attached side of the coverslip was then covered in filtered deionized water, inverted to create a hanging drop and imaged by confocal

microscopy as detailed below, using an 63× 1.2 NA violet-corrected Plan Apochromatic water-immersion objective (Nikon Instruments, Melville, NY).

Confocal microscopy

Live cells grown on 14-mm glass-bottomed 35-mm dishes (Mattek) precoated with poly-*d*-lysine were washed with PBS and observed in the same solution. Imaging was performed at room temperature on an Eclipse C1si laser-scanning confocal microscope (Nikon Instruments) equipped with a 63×, 1.4 NA, violet-corrected plan Apochromatic oil objective and a multianode photomultiplier tube with 32 channels (both by Nikon Instruments). The meCFP, meYFP, and DsRed2 fluorescence signals were acquired by 439-, 514-, and 561-nm excitation, respectively. Where required, images were linearly unmixed with the EZ-C1 software (Nikon Instruments) for the emission spectra of the fluorophores of interest, using reference spectra individually compiled for each fluorophore expressed in the same cell type.

Donor recovery after acceptor photobleach FRET

A series of λ-stack *X-Y* images were collected with the Eclipse C1si laser-scanning confocal microscope (Nikon Instruments). Dequenching of meCFP fluorescence during incremental photobleaching of meYFP was performed and analyzed as described previously in Son et al. (24) and Nashmi et al. (25). Donor recovery after acceptor photobleach (DRAP) Förster resonance energy transfer (FRET) efficiency (E) was calculated as

$$E = 1 - \left(\frac{I_{DA}}{I_D}\right). \tag{1}$$

Here, I_{DA} represents the normalized fluorescence intensity of meCFP (100%) in the presence of nonbleached acceptor. I_D represents the normalized fluorescence intensity of meCFP after 100% photobleach of I_A, the acceptor meYFP. The I_D value was extrapolated from a scatter plot of the percentage increase of meCFP fluorescence versus the percentage decrease of meYFP fluorescence for each cell (as seen later in Figs. 4 and 5 *C*) (25).

Fluorescence intensity ratio

First described by Zheng and Zagotta (26) in 2004, fluorescence intensity ratios (FIR) allow the pairwise determination of the relative abundance of proteins (27,28). This is achieved by labeling both proteins of interest with each of two fluorescent reporters. Given reporter requirements for complete and stoichiometric labeling and the desire to minimize fluorophore-specific changes in target expression, fluorescent protein fusions utilizing the highly homologous meCFP and meYFP are typically chosen.

In FIR, all of the photophysical particularities of the instrumental setup and the chosen fluorescent proteins reside within a coefficient (C) that relates observed fluorescence intensities to the relative abundance of the receptor subunits to which they are fused.

For AmeCFP BmeYFP, this relationship is

$$k_1 = \frac{I_{\text{meCFP}}}{I_{\text{meYFP}}} = C \times \left(\frac{[A]}{[B]}\right), \tag{2}$$

and for AmeYFP BmeCFP, this relationship is

$$k_2 = \frac{I_{\text{meCFP}}}{I_{\text{meYFP}}} = \frac{C}{\left(\frac{[A]}{[B]}\right)}. \tag{3}$$

Having determined the fluorescence intensity ratios for fluorescent protein-receptor subunit fusion pairs, one rearranges the above equations to yield both $[A]/[B]$ and C as follows:

$$\left(\frac{[A]}{[B]}\right) = \sqrt{\frac{k_1}{k_2}}, \tag{4}$$

$$C = \sqrt{k_1 \times k_2}. \tag{5}$$

One complication resides in the ability of meCFP and meYFP to FRET. However, as a ratiometric method, donor intensity loss via FRET is expected to affect FIR only to the extent that FRET efficiency differs between the two fluorescent protein fusion pairs. When such a difference in FRET efficiency occurs, and before the acceptor is photobleached, a correction factor (d_0) to predict the direction and degree of change in subunit ratio can be calculated by Eqs. 6 and 7, where E_1 is the FRET efficiency for $A_{\text{meCFP}}B_{\text{meYFP}}$ and E_2 is that for $A_{\text{meYFP}}B_{\text{meCFP}}$:

$$d_0 = \sqrt{\frac{\left(1/1 - E_2\right)}{\left(1/1 - E_1\right)}}, \tag{6}$$

$$\text{Corrected}\left(\frac{[A]}{[B]}\right)_0 = d_0 \times \left(\left(\frac{[A]}{[B]}\right)_0\right). \tag{7}$$

To calculate FIR, we always used the acceptor intensity at the beginning of the experiment, before any acceptor photobleaching (shown later in Tables 4 and 5, $I_{\text{meYFP}} = 1$). Note that these later-appearing tables, Tables 4 and 5, contain experimental values for d_0. Figs. 4 and 5 *B*, also shown later, provide examples of this progression.

The constant C varied by ±20% among our experiments performed on different days. This was determined both through calculation of C in FIR measurements and tests of the predictive power of that value, including one using equal mole fractions of 5-HT$_3$A-meYFP and 5-HT$_3$A-meCFP cDNA and unlabeled 5-HT$_3$B, and another using unlabeled 5-HT$_3$A and equal mole fractions of 5-HT$_3$B-meYFP and 5-HT$_3$B-meCFP cDNA. Possible bases for this variation include uncontrolled, small changes in oxygenation, temperature, or the cell cycle, any of which may change the fraction of immature (i.e., dark) fluorophores.

RESULTS

Fusion constructs of the human 5-HT$_3$A and 5-HT$_3$B subunits with fluorescent proteins were generated. Both meCFP and meYFP were individually added to the 5-HT$_3$A and 5-HT$_3$B subunits, allowing both combinations of the two fluorescent proteins to be probed. As with previous Cys-loop receptor subunits, the fluorescent protein was introduced into the M3-M4 intracellular loop, taking care to avoid known phosphorylation and trafficking motifs (2,25,29). These constructs were then transiently expressed in HEK293T cells, and their functional response to serotonin was assayed using a voltage-sensitive dye. The 5-HT$_3$AB receptors formed from the fluorescent protein fusion constructs show maximal responses, EC_{50} values, and Hill coefficients essentially equivalent to the unlabeled receptor (Fig. 1; Table 1). This suggests that neither fluorescent label perturbs the expression level or function of the hetero-pentameric 5-HT$_3$ receptor. The characteristic shifts in EC_{50}

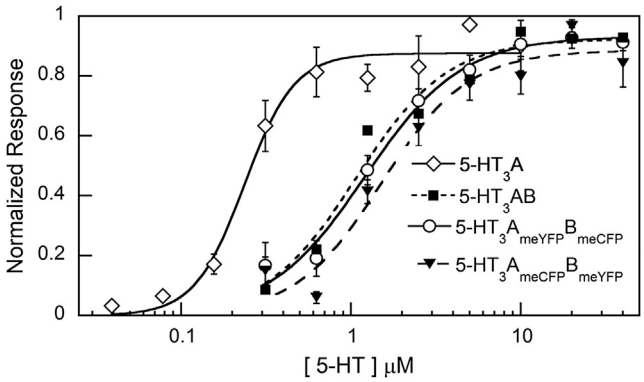

FIGURE 1 5-HT$_3$ receptor agonist dose-response relations are not changed by labeling the fluorescent labels on the subunits. Receptors expressed in HEK293T cells were assayed with a voltage-sensitive dye. All heteromeric receptors were transfected with a 1:1 ratio of A/B subunit cDNA. See Table 1.

and Hill coefficient between the homo- and heteromeric receptors would betray mixed populations of receptor by generating a biphasic dose-response relationship. An equal mole ratio of transfected 5-HT$_3$A and 5-HT$_3$B subunit DNA, however, yielded a pure population of heteromeric receptors.

Transfected fluorescent 5-HT$_3$ receptor and ER marker showed extensive colocalization, demonstrating marked ER retention of the component receptor subunits, thereby obscuring the plasma membrane population of assembled functional receptors (Fig. 2). The ER retention seen with transfected cells may be partially due to the addition of the large GFP proteins. To isolate plasma membrane-embedded receptors, plasma membranes were allowed to adhere to a coverslip before being mechanically sheared away from the cell body by removal of that coverslip. Extensive rinsing in PBS removed residual intracellular contents. Subsequent imaging of the coverslip reveals much lower ER marker fluorescence while retaining fragments bearing fluorescent 5-HT$_3$ receptor with shallow z-axis signatures. We term these "membrane sheets".

FIR measurements show A_3B_2 subunit ratios

FIR measurements (Fig. 3) provide direct determination of subunit ratios. As will be shown below, these measurements required only minimal correction for FRET. FIR were determined for membrane sheets containing both labeling patterns (5-HT$_3$A-meYFP/5-HT$_3$B-meCFP and 5-HT$_3$A-meCFP/5-HT$_3$B-meYFP; see Fig. S1 in the Supporting Material). The average FIR for both pairings of subunit and fluorescent protein were then related by Eq. 4 to yield the relative concentration of A to B subunits (Table 2). The membrane-sheet/subunit ratio revealed by FIR shows a slight dependence on the cDNA transfection ratio, but in all cases strongly suggests three A subunits for every two B subunits (Fig. 3).

TABLE 1 5-HT$_3$ Receptor agonist dose-response data

	Maximal response (AU)	5-HT EC_{50} (μM)	Hill coefficient (n_H)	N
5-HT$_3$A	667 ± 28	0.24 ± 0.02	3.0 ± 0.6	16
5-HT$_3$AB	616 ± 23	1.1 ± 0.2	1.8 ± 0.3	6
5-HT$_3$A$_{meYFP}$B$_{meCFP}$	574 ± 31	1.2 ± 0.1	1.5 ± 0.2	6
5-HT$_3$A$_{meCFP}$B$_{meYFP}$	571 ± 54	1.5 ± 0.3	1.7 ± 0.4	6
5-HT$_3$AB$_{Y129S}$	526 ± 23	1.3 ± 0.1	1.8 ± 0.3	6

All values are reported as mean ± standard error.

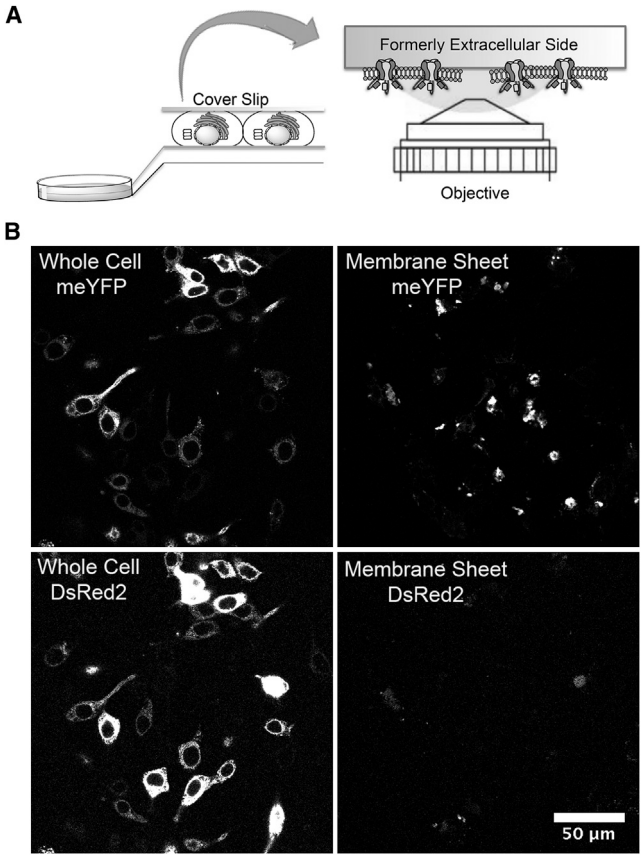

FIGURE 2 Fluorescence imaging of whole cells and isolated membrane sheets. (*A*) Illustration of membrane-sheet preparation method. (*B*) HEK293T cells transfected with 5-HT$_3$A$_{meYFP}$ and DsRed2-ER.

Clearly, the ratio of subunit cDNA transfected did not strongly influence the ratio of subunit protein expressed in the plasma membrane sheets. When similar analyses were performed on intact cells, we found a markedly different pattern. Although 2–3 day incubations were required for satisfactory fluorescence signals in the membrane-sheet samples, strong fluorescence was observed within 24 h of transfection for whole cells. In identically treated samples transfected with 0.75 mol fraction 5-HT$_3$B, the whole cell fluorescence intensity corresponding to the A subunit increased 7.5 ± 1.2-fold from membrane-sheet levels. The fluorescence intensity corresponding to the B subunit increased only 3.5 ± 0.5-fold. The subunit ratios calculated

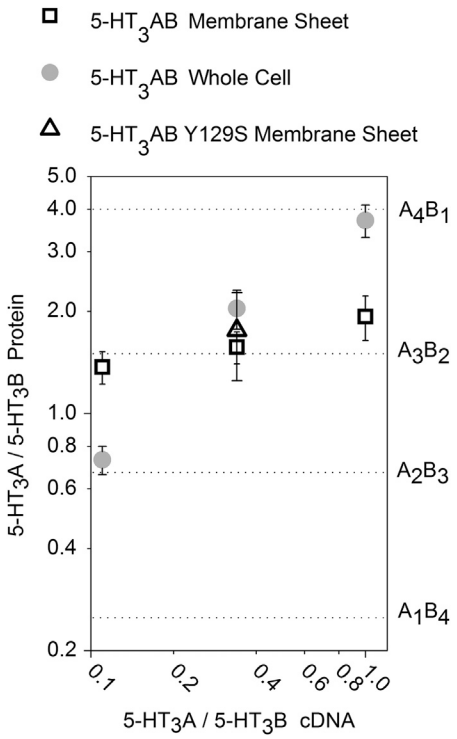

FIGURE 3 5-HT$_3$AB receptor subunit ratio is 3:2 on the plasma membrane, as calculated by FIR at various subunit cDNA transfection ratios. Both axes are shown on a logarithmic scale. See Table 2. Error bars depict the standard error.

by FIR were strongly dependent on the relative amount of subunit cDNA transfected. Whereas the membrane-sheet subunit ratios all suggest a single receptor subunit ratio, in whole cells every condition points toward a different ratio (Fig. 3; Table 3).

Family FRET measurements provide minor corrections to FIR and support for A_3B_2 stoichiometry

Previous work with other heteromeric Cys-loop receptors, especially $\alpha4\beta2$ nicotinic receptors, has shown that fluorescently labeled heteromeric receptors of differing stoichiometries can display differences in FRET efficiencies (24,30). The FIR experiments described in Fig. 3 provide a family FRET experiment: all the A subunits bear donor fluorophores, and all the B subunits bear acceptor fluorophores (or vice versa). To evaluate family FRET efficiencies, DRAP time courses were determined (Fig. 4, *A–C*). Donor fluorescence at complete acceptor photobleach is extrapolated from this time course, allowing for the calculation of FRET efficiency by Eq. 1. This procedure was performed for both pairings of subunit and fluorescent protein within the heteromeric receptor at various transfected mole ratios of 5-HT$_3$A and 5-HT$_3$B subunit cDNA (Table 2). The stoichiometry of donor fluorophores to acceptor fluorophores is different in the two pairings of subunit and fluorescent protein. This causes changes in the measured FRET efficiencies of CFP- and YFP-labeled 5-HT$_3$AB receptors in the membrane sheets.

In a first application of these family FRET measurements, we employed them in Eqs. 6 and 7 to calculate the correction factor (d_0) to the FIR measurements.

In a second application of these family FRET measurements, their comparative amplitudes provide independent support for our conclusions about subunit stoichiometry.

A satisfactory theory for family FRET measurements must account for several factors, including the subunit order, dipole orientation, departures from pentameric symmetry, and coplanarity of the fluorophores within the M3-M4 loops (24,30). These parameters are not known for any heteromeric Cys-loop receptor. Importantly, a reasonable range of assumptions about these parameters predict that FRET for two donor subunits and three acceptor subunits exceeds that for a receptor with three donor subunits and two acceptor subunits (24,30). The theory accounts for published data on transfected cells in which $\alpha4\beta2$ stoichiometries were manipulated in one of three ways:

1. By varying fluorescent subunit cDNA ratios;
2. By treating with pharmacological chaperone; or
3. By mutations that change the stoichiometry (30,31).

These experiments on 5-HT$_3$AB showed the pattern expected from the FIR data (24,30). 5-HT$_3$AB receptors thought to have two donors/three acceptors from the FIR data had greater FRET than those with three donors/two acceptors. When the A subunit was labeled with the acceptor

TABLE 2 Fluorescence data, membrane sheets

Mole fraction 5-HT$_3$A		Mole fraction 5-HT$_3$B		FRET	Fluorescence intensity		
meCFP	meYFP	meCFP	meYFP	efficiency (%)	ratio (meCFP/meYFP)	[A]/[B]	*N*
0.5			0.5	26.1 ± 0.7	0.273 ± 0.023	1.93 ± 0.29	22
	0.5	0.5		30.8 ± 0.4	0.073 ± 0.009		16
0.25			0.75	27.6 ± 0.6	0.231 ± 0.015	1.57 ± 0.17	44
	0.25	0.75		32.7 ± 0.8	0.094 ± 0.008		40
0.1			0.9	25.2 ± 0.6	0.190 ± 0.015	1.37 ± 0.15	13
	0.1	0.9		33.9 ± 1.4	0.102 ± 0.009		21

All values are reported as mean ± standard error.

TABLE 3 Fluorescence data, whole cells

Mole fraction 5-HT$_3$A		Mole fraction 5-HT$_3$B		FRET efficiency (%)	Fluorescence intensity ratio (meCFP/meYFP)	[A]/[B]	*N*
meCFP	meYFP	meCFP	meYFP				
0.5			0.5	15.7 ± 0.5	0.618 ± 0.047	3.71 ± 0.41	23
	0.5	0.5		57.8 ± 5.0	0.045 ± 0.003		24
0.25			0.75	26.8 ± 1.2	0.424 ± 0.025	2.04 ± 0.27	25
	0.25	0.75		47.5 ± 2.2	0.102 ± 0.012		17
0.1			0.9	32.5 ± 0.7	0.135 ± 0.011	0.73 ± 0.07	20
	0.1	0.9		21.7 ± 1.2	0.252 ± 0.017		24

All values are reported as mean ± standard error.

(meYFP) and the B subunit with the donor (meCFP), FRET efficiency was 1.18–1.34 times that with the opposite pairing when evaluating membrane sheets. The FRET efficiency was also independent of cDNA transfection ratio. These data are consistent with the view of a receptor with an A_3B_2 stoichiometry on the plasma membrane. In contrast, the FRET efficiencies for whole cells were strongly dependent on cDNA transfection ratio (Fig. 4, *D* and *E*; Table 3).

In the absence of a correction for the higher FRET efficiency when the A subunit has meYFP, the ratio of A/B subunits derived from FIR (detailed previously) varies at different degrees of acceptor photobleaching. Furthermore,

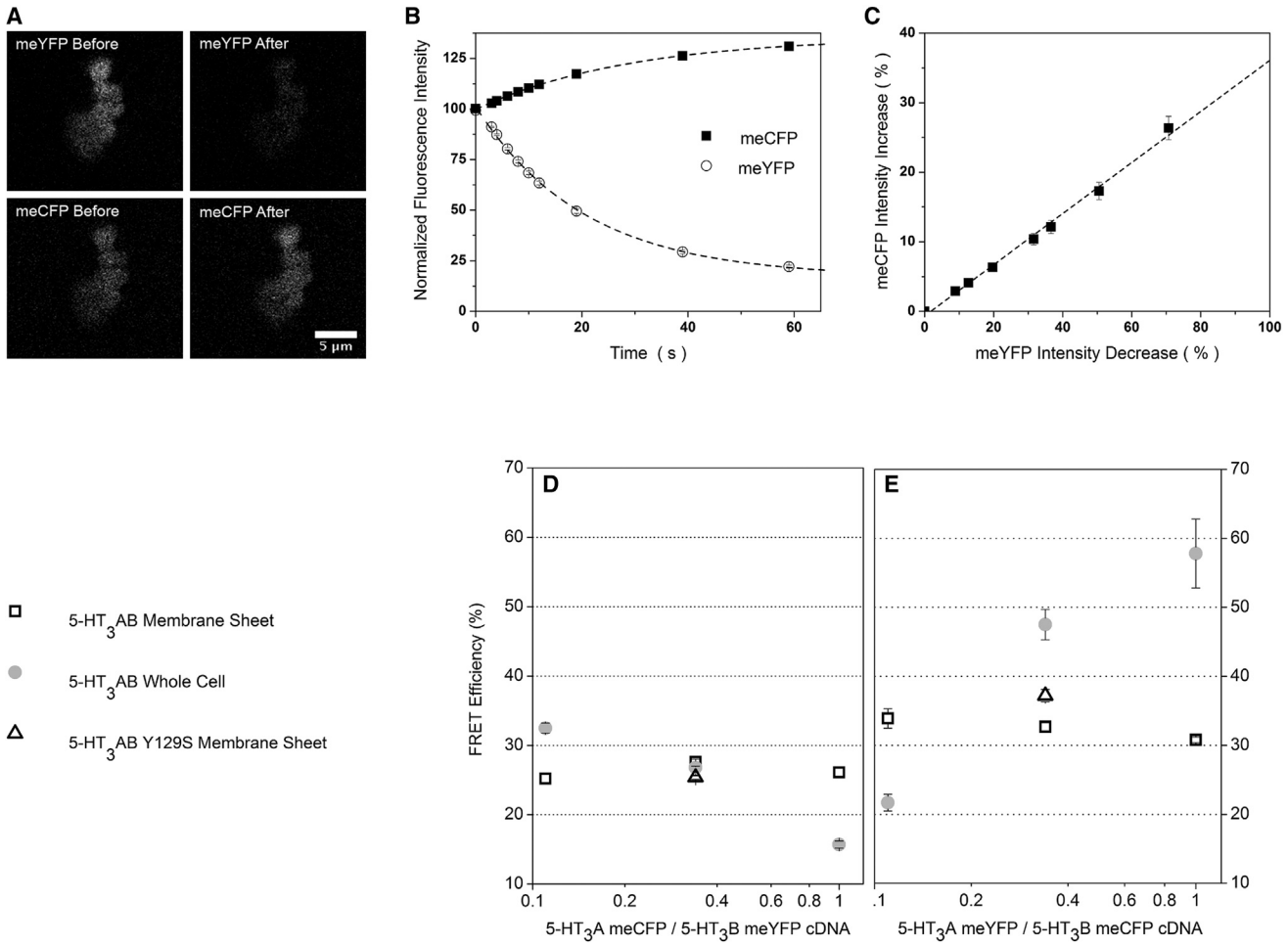

FIGURE 4 Family FRET measurements are consistent with A_3B_2 stoichiometry. Donor recovery after acceptor photobleaching (DRAP) on 5-HT$_3$AB membrane sheets. (*A*) Representative membrane-sheet images before and after photobleaching for $A_{meCFP}B_{meYFP}$ transfected with a 1:1 ratio of A/B subunit cDNA. (*B*) The corresponding plot of fluorescence during the acceptor photobleaching time course. (*C*) Extrapolation of the photobleaching time course in B to donor fluorescence intensity at complete acceptor bleach. (*D*) FRET efficiency of 5-HT$_3A_{meYFP}B_{meCFP}$ at various subunit cDNA transfection ratios. The *X* axis is shown on a logarithmic scale. (*E*) FRET efficiency of 5-HT$_3A_{meCFP}B_{meYFP}$ at various subunit cDNA transfection ratios. The *X* axis is shown on a logarithmic scale. See Table 2. Error bars depict the standard error.

if both measures are exclusively the result of assembled receptors, the difference in FRET efficiencies should predict the direction and degree of change in the subunit ratio according to Eqs. 6 and 7. For membrane sheets, the changes in subunit ratios derived from FIR during photobleaching agree with the corrected FIR at all cDNA transfection ratios (Table 4).

For whole cells, the d_0-corrected subunit ratio is markedly different from that observed at complete acceptor photobleach for two of three transfection ratios (Table 5). This indicates that additional complexities contribute to the FRET efficiencies and subunit ratios for whole cells.

Twin FRET measurements support the inference of A_3B_2 stoichiometry

We also employed another FRET-based method for probing stoichiometry—twin FRET analysis—in which receptors are composed of one subunit subtype that is unlabeled and another that is an equal mixture of CFP and YFP constructs (24) (Fig. 5, *A–D*). Previous theory and experiments show that twin FRET data for $(\alpha4)_3(\beta2)_2$ versus $(\alpha4)_2(\beta2)_3$ nAChRs are dominated by the fact that the former stoichiometry has two adjacent $\alpha4$ subunits and no adjacent $\beta2$ subunits; but the latter stoichiometry has the contrasting pattern of adjacency. The differences arise from the steep distance-dependence of FRET (24).

Membrane sheets transfected with 0.75 mol fraction 5-HT$_3$B with the A subunit doubly labeled have a FRET efficiency of 33.2 ± 1.2% (N = 19) (Fig. 5 *D*). This is generally compatible with a structure containing at least two A subunits. The rather high efficiency suggests that two of the A subunits are adjacent in most receptors; this is required if there are three A subunits in a pentamer.

Twin FRET between the labeled B subunits is also detectable, at an efficiency of 18.3 ± 0.7% (N = 9) (Fig. 5 *D*). This shows that there are also at least two B subunits. As discussed below, the lower FRET efficiency for the B subunits indicates that probably there are only two, nonadjacent B subunits in most receptors. Thus, these twin FRET experiments also support the conclusion of predominantly A_3B_2 stoichiometry.

The 5-HT$_3$B Y129S subunit assembles into receptors like the B subunit

The B subunit studied in the experiments above contains tyrosine at position 129. A single-nucleotide nonsynonymous polymorphism *HTR3B* p.Y129S (c.386A>C, rs11767445) has been associated with several diseases, including major depression and bipolar affective disorder (4,32–34). This residue is located on a β-strand beneath the orthosteric binding site, and the side chain is modeled to project into the inter-subunit interface. We constructed and studied Y129S subunits containing both fluorophores.

To investigate the possibility that Y129S might affect receptor assembly and stoichiometry, the subunit ratio determined by FIR was measured on membrane sheets transfected with 0.75 mol fraction 5-HT$_3$B$_{Y129S}$. The FRET efficiencies and subunit ratio calculated by FIR were largely unchanged from that of the Y129 B subunit (which we usually term B) receptor, suggesting a receptor stoichiometry of three A subunits and two B subunits for the variant receptor (Tables 2 and 6; Fig. 3; Fig. 4, *D* and *E*).

Because heterozygotes for the B subunit allele (one 129Y, one 129S) occur in >30% of many human populations (32), we investigated the relative efficiency of incorporating the two variant B subunits, when both are expressed simultaneously. In the conceptually simplest experiments (Table 7), we directly compared the plasma membrane subunit ratios of tagged Y129 B (also called simply, B) subunits and tagged B$_{Y129S}$ subunits when those cDNAs were transfected at equal amounts, along with labeled A subunit cDNAs. We found a [B]/B$_{Y129S}$ ratio of 0.86 ± 0.12. Twin FRET efficiencies between coassembled B and B$_{Y129S}$ subunits (17–19%) are near those between coassembled B and B subunits (18%) (Fig. 5 *D* and Table 7).

In another experiment (Table 8), untagged B subunits and tagged B$_{Y129S}$ subunits were expressed at equal cDNA amounts, along with tagged A subunits. We measured a plasma membrane [A]/B$_{Y129S}$ subunit ratio of 2.66 ± 0.37, implying that B$_{Y129S}$ subunits are 1.11-fold more abundant than the value of 3 expected if the two B subunit variants incorporated with equal efficiency in A_3B_2 receptors. Family FRET experiments gave additional information. With B$_{Y129S}$-meYFP as acceptor, we measured a FRET efficiency of 12.4 ± 0.2%, as expected if each receptor has roughly half as many B-acceptors. With B$_{Y129S}$-meCFP as donor, we measured a FRET efficiency like that in previous experiments, suggesting that, as usual, each B subunit donor resides in a receptor with three A subunit acceptors.

Thus the FIR experiments show a consistent pattern. When the two subunit variants are expressed simultaneously, the B$_{Y129S}$ subunit incorporates into assembled

TABLE 4 Effect of acceptor photobleaching on subunit ratio, membrane sheets

Mole fraction 5-HT$_3$B	I_{meYFP} = 1	I_{meYFP} = 0.6	I_{meYFP} = 0.25	I_{meYFP} = 0	d_0	I_{meYFP} = 1 corrected by d_0
0.5	1.96 ± 0.31	1.95 ± 0.29	1.97 ± 0.28	1.93 ± 0.29	0.97	1.90
0.75	1.60 ± 0.19	1.58 ± 0.19	1.56 ± 0.17	1.57 ± 0.17	0.96	1.54
0.9	1.41 ± 0.20	1.38 ± 0.18	1.36 ± 0.15	1.37 ± 0.15	0.94	1.33

All values are reported as mean ± standard error.

TABLE 5 Effect of acceptor photobleaching on subunit ratio, whole cells

Mole fraction 5-HT$_3$B	$I_{meYFP} = 1$	$I_{meYFP} = 0.6$	$I_{meYFP} = 0.25$	$I_{meYFP} = 0$	d_0	$I_{meYFP} = 1$ corrected by d_0
0.5	4.84 ± 0.68	4.09 ± 0.53	3.59 ± 0.50	3.71 ± 0.41	0.71	3.42
0.75	2.17 ± 0.37	2.09 ± 0.31	2.05 ± 0.27	2.04 ± 0.27	0.85	1.84
0.9	0.68 ± 0.07	0.71 ± 0.08	0.72 ± 0.08	0.73 ± 0.07	1.08	0.73

All values are reported as mean ± standard error.

plasma membrane 5-HT$_3$AB receptors in a manner slightly (1.11–1.14-fold) more efficient than that of the B subunit.

DISCUSSION

These measurements provide a robust determination of subunit stoichiometry for a Cys-loop receptor in the plasma membrane. The data arise from combining several techniques, including isolation of plasma membrane sheets (23), FIR measurements (26–28), FRET measurements, and the placement of fluorescent proteins in the M3-M4 loop of Cys-loop receptors while conserving most aspects of receptor function (24,25). Heteromeric receptors formed from subunits containing fluorescent proteins display minimally perturbed serotonin EC$_{50}$ values and Hill coefficients in HEK293T cells (Fig. 1; Table 1).

In whole cells, retention of the receptor subunits in the endoplasmic reticulum complicated the characterization of assembled receptors on the plasma membrane. In particular, subunit ratios determined by various approaches are strongly dependent on cDNA transfection ratios. This suggests that unassembled and partially assembled subunits in the ER dominate the calculation, as might be expected given the observed subunit ER retention (Fig. 2). We also observe an overabundance of the A subunit relative to its cDNA proportion, which is likely due to the previously reported endoplasmic reticulum-associated degradation of the B subunit (35).

To circumvent this problem, the membrane was isolated by glass adhesion and mechanical shearing (Fig. 2) (35,36). Following this procedure, appearance of ER marker is sharply reduced, while patches of membrane-containing receptor termed "membrane sheets" remain. All efforts to characterize the stoichiometry of receptors employed membrane sheets.

FIR were constructed for each membrane sheet using FRET-corrected fluorescence intensities. Average values were calculated for each pairing of fluorescent protein and receptor subunit at each cDNA transfection ratio (Tables 2 and 3; Fig. 3). The relative amount of each subunit was then extracted by Eq. 4. Studies of membrane sheets are

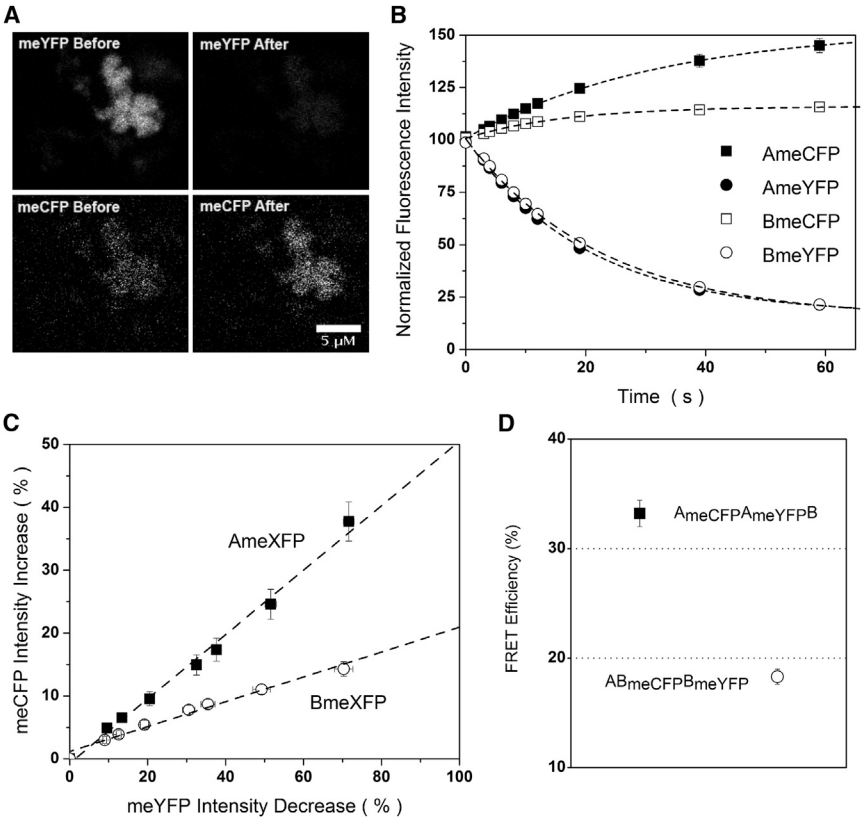

FIGURE 5 Twin FRET measurements are consistent with A_3B_2 stoichiometry and with nonadjacent B subunits. Donor recovery after acceptor photobleaching (DRAP) on 5-HT$_3$AB membrane sheets. (*A*) Representative membrane-sheet images before and after photobleaching for $A_{meCFP}A_{meYFP}B$ transfected with a 1:1:6 ratio of A_{meCFP}/A_{meYFP} to untagged B subunit cDNA. (*B*) Plot of fluorescence during the acceptor photobleaching time course for both tagged A or tagged B subunit 5-HT$_3$AB twin FRET experiments. (*C*) Extrapolation of the photobleaching time courses in B to donor fluorescence intensity at complete acceptor bleach. (*D*) Twin FRET efficiencies of tagged A or tagged B subunit 5-HT$_3$AB receptors. Error bars depict the standard error.

TABLE 6 5-HT$_3$AB$_{Y129S}$ membrane-sheet fluorescence data for A and B

Mole fraction 5-HT$_3$A		Mole fraction 5-HT$_3$B$_{Y129S}$		Family FRET	Fluorescence intensity		
meCFP	meYFP	meCFP	meYFP	efficiency (%)	ratio (meCFP/meYFP)	[A]/[B$_{Y129S}$]	*N*
0.25			0.75	25.4 ± 0.3	0.309 ± 0.083	1.76 ± 0.51	13
	0.25	0.75		37.2 ± 0.9	0.100 ± 0.010		20

All values are reported as mean ± standard error.

rather consistent in their support for an A_3B_2 subunit ratio (Fig. 3 *A*). The FIR at 0.5 mol fraction 5-HT$_3$A is, however, significantly different from the expected value for this stoichiometry. There are two possible explanations:

1. This deviation could arise from a small population of homomeric 5-HT$_3$A receptors. This is supported by the whole-cell subunit ratio at this transfection condition, which shows nearly four A subunits per B subunit expressed. While a monophasic dose-response curve for serotonin is seen at this transfection ratio (Fig. 1), the markedly higher single channel conductance of the 5-HT$_3$AB receptor (16–30 pS versus sub-pS for 5-HT$_3$A) allows it to obscure even moderate proportions of homomeric receptor (7).
2. The membrane-sheet preparation could retain a small amount of intracellular receptors, perhaps in organelles, again distorting the measurements (Fig. 1).

FIR measurements do not formally rule out the possibility that the data arise in part from isolated groups of A subunits and B subunits, because the groups would be separated by less than the resolution of the microscope. FRET measurements, however, present the advantage that the FRET efficiencies depend on donor-acceptor interactions within assembled pentamers.

The family FRET efficiencies between receptor subunits within these membrane sheets were determined for various ratios of transfected subunit cDNA by monitoring DRAP (Fig. 4, *A–C*). Unlike those in whole cells, the FRET efficiencies in membrane sheets are nearly independent of subunit cDNA transfection ratio (Table 2; Fig. 4, *D* and *E*). This supports the contention of the FIR measurements that membrane sheets are enriched in a single population of assembled membrane receptors, evidenced as loose donor subunits generated by biased transfection-decrease FRET efficiency.

The FRET efficiency of 5-HT$_3$A$_{meYFP}$B$_{meCFP}$ was 1.18–1.34-fold (average of 1.24-fold) greater than that for the opposite pairing of fluorescent protein and receptor subunit. Previous theoretical and experimental studies on other members of the Cys-loop receptor family have determined that this difference in FRET efficiency is consistent with a receptor stoichiometry of A_3B_2 (24,30). These analyses, summarized in the Supporting Material (see Fig. S2), depend on the ratio of donors/acceptors imposed by a pentameric receptor and the proportion of couplings between adjacent/nonadjacent receptor subunits.

The FRET measurements present the disadvantage that conclusions cannot be made about the actual physical distance between the fluorophores, because one does not know many factors, including the subunit order, dipole orientation, departures from pentameric symmetry, and coplanarity of the fluorophores within the M3–M4 loops. The measured FRET efficiencies would be compatible with a wide range of assumptions about these parameters, if adjacent subunits have a fluorophore separation of 30–45 Å. This distance is broadly consistent with known Cys-loop receptor structures (30).

Further support that the membrane sheets correspond to purified plasma membrane containing assembled receptors is found by analyzing the effect of acceptor photobleaching on the calculated subunit ratios. The observed difference in FRET efficiencies between the two pairs of fluorescent proteins and receptor subunits described earlier can be used to generate a correction factor, d_0 (Eq. 6). The value d_0 can then be used to predict the direction and magnitude of the change in calculated subunit ratio upon acceptor photobleaching (Eq. 7). This prediction will fail if loose or partially assembled subunits sway the subunit ratio without FRET, or if they contribute inordinately to FRET by aggregating, as is observed in whole cells (Table 4). In membrane sheets the correction factor correctly predicts subunit ratios under every condition (Table 5).

Additional information about stoichiometry and subunit order is found in twin FRET experiments on membrane sheets (Fig. 5). With this technique, the FRET between two subunits of the same subtype is monitored. The existence of twin FRET between A subunits, and in another

TABLE 7 5-HT$_3$AB$_{Y129S}$ membrane-sheet FIR data for A and B

Mole fraction 5-HT$_3$A		Mole fraction 5-HT$_3$B$_{Y129S}$		Family FRET	Fluorescence intensity		
meCFP	meYFP	meCFP	meYFP	efficiency (%)	ratio (meCFP/meYFP)	[A]/[B$_{Y129S}$]	*N*
0.25			0.375	12.4 ± 0.2	0.466 ± 0.049	2.66 ± 0.37	19
	0.25	0.375		36.0 ± 0.5	0.066 ± 0.006		20

All values are reported as mean ± standard error. All conditions contain 0.375 mol fraction unlabeled 5-HT$_3$B.

TABLE 8 5-HT$_3$A(BY129 and BS129) membrane-sheet fluorescence data

Mole fraction 5-HT$_3$B		Mole fraction 5-HT$_3$B$_{Y129S}$		Twin FRET	Fluorescence intensity		
meCFP	meYFP	meCFP	meYFP	efficiency (%)	ratio (meCFP/meYFP)	[B]/[B$_{Y129S}$]	*N*
0.375			0.375	17.2 ± 0.3	0.104 ± 0.007	0.86 ± 0.10	16
	0.375	0.375		19.4 ± 0.5	0.140 ± 0.013		16

All values are reported as mean ± standard error. All conditions contain 0.25 mol fraction unlabeled 5-HT$_3$A.

preparation between B subunits, is consistent with a receptor stoichiometry containing at least two A subunits and at least two B subunits. The markedly higher efficiency of the FRET between A subunits, compared to that between B subunits, suggests that most individual 5-HT$_3$AB receptor molecules have an A-A subunit interface but no adjacent B subunits. Pentameric receptors with an A_3B_2 stoichiometry, as suggested by FIR and FRET experiments, must contain at least one A-A subunit interface.

We can provide a more-quantitative interpretation of the twin FRET efficiencies in light of previous theoretical and experimental studies on $\alpha_4\beta_2$ nicotinic acetylcholine receptors (24). In $\alpha_4\beta_2$ receptors, known subunit stoichiometries and known subunit orders on the plasma membrane can be generated by varying cDNA transfection ratios. In a receptor with two α_4 subunits, they are nonadjacent; and in a receptor with two β_2 subunits, they too are nonadjacent. The twin FRET ratio between adjacent and nonadjacent subunits is 1.80 ± 0.21, nearly identical to that found here (1.81 ± 0.10) for A twin FRET versus B twin FRET efficiencies. The agreement between these two analogous experiments on Cys-loop receptors suggests that the 5-HT$_3$AB receptor has subunit order of A-A-B-A-B, that is, one lacking a B-B interface and analogous to an α4-α4-β2-α4-β2 nAChR. This order, in which A-B assembly precludes B-B interactions, is intuitively consistent with previous knowledge that B subunits assemble and traffic to the membrane only upon coexpression with the A subunit.

A synonymous polymorphism in the *HTR3B* gene results in either the more common allele, encoding tyrosine-129, or a modestly less common allele encoding serine. The serine allele is linked to several disorders, including major depression and bipolar affective disorder (32–34). While the serine allele increases 5-HT-induced responses by extending the duration of channel opening (32–34), its complete effects on channel function remain poorly defined. Because the polymorphic residue lies on a β-strand just below the proposed orthosteric ligand-binding site where it may project into the inter-subunit space, we considered the possibility that the side chain affects heteromeric receptor assembly. The 5-HT$_3$AB receptors containing only the B$_{Y129S}$ subunit, however, display a subunit ratio and FRET efficiencies consistent with those observed for the more common B subunit variant (Fig. 3; Fig. 4, *D* and *E*). Thus the B$_{Y129S}$ subunit's profoundly altered gating characteristics (32–34) occur within the usual A_3B_2 receptor structure.

Heterozygotes for the B subunit common allele (one 129Y, one 129S) occur in >30% of many human populations (32), prompting additional experiments to study the 5-HT$_3$AB receptors that would be produced in a heterozygote. We directly compared the efficiency of incorporation of the common and minor variant B subunit by transfecting cells with the A subunit cDNA plus a mixture of cDNAs for these two B subunits. Under the conditions of our experiments, two types of FIR data show that 5-HT$_3$B-Y129S subunit incorporates slightly (1.11–1.14-fold) more efficiently than the 5-HT$_3$B-Y129 subunit (Table 4). In an individual pentamer containing both B subunit alleles, FRET efficiencies between the two B subunits suggest that this heterozygote pentamer has the same stoichiometry and subunit order as a pentamer containing only major alleles of the B subunit (Fig. 5 *D* and Table 7).

Our experiments perform a quantitative analysis of heteropentameric receptors with only two types of subunits. They require modest equipment and minimal assumptions. The methods do require moderately high levels of plasma membrane protein density, probably >100/μm^2. In future studies, the membrane-sheet isolation procedure will allow more-precise information on Cys-loop receptors with more complex compositions in the plasma membrane; such receptors would include nAChR, GABA$_A$, and some invertebrate Cys-loop receptors. This can be accomplished through the accumulation of pairwise subunit relative abundances or through employing modern available fluorophores, and modern spectrally resolved microscopes, that enable one to detect three fluorophores in a given membrane sample. One can readily permute fluorophores among three subunit types, leading to six FIR experiments. This would provide redundant, consistent determinations of subunit ratios.

Previous reports have shown how pairwise family FRET experiments provide qualitative proof that individual pentameric receptors contain three types of nAChR subunits (α4β2β3, α4α6β2, α6β2β3) or four types of nAChR subunits (α4, α6, β2, β3) (37). In twin FRET experiments, the β3 subunit, where present, displays near-zero twin FRET and therefore exists as only one copy per pentamer. In contrast, the other tested subunits have >1 copy in at least some individual nAChR molecules (37). It would therefore be possible to determine subunit ratios, stoichiometry, and order in pentameric Cys-loop receptors containing three, four, or even five (38) subunit types. Thus, the straightforward combination of membrane-sheet isolation, FIR, family FRET, and twin FRET is a generally promising procedure

for determining subunit ratios, stoichiometry, and subunit order of proteins on the plasma membrane.

CONCLUSIONS

Previous reports have supported two different possible stoichiometries for the 5-HT_3AB receptor. In this work, we have utilized a method to isolate plasma membrane sheets containing assembled receptors and used this to determine the stoichiometry of the 5-HT_3AB receptor by fluorescence methods: FIR, family FRET, and twin FRET. Our strongest, non-model-dependent conclusion arises from FIR, which shows an A_3B_2 subunit ratio. Family FRET and twin FRET efficiencies are also consistent with an A_3B_2 stoichiometry.

SUPPORTING MATERIAL

Two figures and additional narrative paragraphs are available at http://www.biophysj.org/biophysj/supplemental/S0006-3495(13)00799-6.

The authors thank Rahul Srinivasan, Kristina N. Daeffler, and Ethan B. Van Arnam for technical assistance and helpful discussion.

This work was supported by grants (No. NS034407, No. DA017279, and No. AG033954) from the National Institutes of Health, Bethesda, MD.

REFERENCES

1. Lummis, S. C. 2012. 5-HT_3 receptors. *J. Biol. Chem.* 287:40239–40245.
2. Thompson, A. J., H. A. Lester, and S. C. Lummis. 2010. The structural basis of function in Cys-loop receptors. *Q. Rev. Biophys.* 43:449–499.
3. Walstab, J., G. Rappold, and B. Niesler. 2010. 5-HT_3 receptors: role in disease and target of drugs. *Pharmacol. Ther.* 128:146–169.
4. Jensen, A. A., P. A. Davies, …, K. Krzywkowski. 2008. 3B but which 3B, and that's just one of the questions: the heterogeneity of human 5-HT_3 receptors. *Trends Pharmacol. Sci.* 29:437–444.
5. Davies, P. A., M. Pistis, …, E. F. Kirkness. 1999. The 5-HT_{3B} subunit is a major determinant of serotonin-receptor function. *Nature.* 397:359–363.
6. Niesler, B., J. Walstab, …, M. Brüss. 2007. Characterization of the novel human serotonin receptor subunits 5-HT_3C,5-HT_3D, and 5-HT_3E. *Mol. Pharmacol.* 72:8–17.
7. Thompson, A. J., and S. C. Lummis. 2013. Discriminating between 5-HT_3A and 5-HT_3AB receptors. *Br. J. Pharmacol.* 169:736–747.
8. Hapfelmeier, G., C. Tredt, …, G. Rammes. 2003. Co-expression of the 5-HT_3B serotonin receptor subunit alters the biophysics of the 5-HT_3 receptor. *Biophys. J.* 84:1720–1733.
9. Stewart, A., P. A. Davies, …, T. G. Hales. 2003. Introduction of the 5-HT_{3B} subunit alters the functional properties of 5-HT_3 receptors native to neuroblastoma cells. *Neuropharmacology.* 44:214–223.
10. Hu, X. Q., and R. W. Peoples. 2008. The 5-HT_3B subunit confers spontaneous channel opening and altered ligand properties of the 5-HT_3 receptor. *J. Biol. Chem.* 283:6826–6831.
11. Das, P., and G. H. Dillon. 2003. The 5-HT_3B subunit confers reduced sensitivity to picrotoxin when co-expressed with the 5-HT_3A receptor. *Brain Res. Mol. Brain Res.* 119:207–212.
12. Baptista-Hon, D. T., T. Z. Deeb, …, T. G. Hales. 2012. The 5-HT_{3B} subunit affects high-potency inhibition of 5-HT_3 receptors by morphine. *Br. J. Pharmacol.* 165:693–704.
13. Kelley, S. P., J. I. Dunlop, …, J. A. Peters. 2003. A cytoplasmic region determines single-channel conductance in 5-HT_3 receptors. *Nature.* 424:321–324.
14. Livesey, M. R., M. A. Cooper, …, J. A. Peters. 2008. Structural determinants of Ca^{2+} permeability and conduction in the human 5-hydroxytryptamine type 3A receptor. *J. Biol. Chem.* 283:19301–19313.
15. Peters, J. A., M. A. Cooper, …, J. J. Lambert. 2010. Novel structural determinants of single channel conductance and ion selectivity in 5-hydroxytryptamine type 3 and nicotinic acetylcholine receptors. *J. Physiol.* 588:587–596.
16. Maricq, A. V., A. S. Peterson, …, D. Julius. 1991. Primary structure and functional expression of the 5HT_3 receptor, a serotonin-gated ion channel. *Science.* 254:432–437.
17. Holbrook, J. D., C. H. Gill, …, M. J. Gunthorpe. 2009. Characterization of 5-HT3C, 5-HT3D and 5-HT3E receptor subunits: evolution, distribution and function. *J. Neurochem.* 108:384–396.
18. Kapeller, J., D. Möller, …, B. Niesler. 2011. Serotonin receptor diversity in the human colon: expression of serotonin type 3 receptor subunits 5-HT3C, 5-HT3D, and 5-HT3E. *J. Comp. Neurol.* 519:420–432.
19. Barrera, N. P., P. Herbert, …, J. M. Edwardson. 2005. Atomic force microscopy reveals the stoichiometry and subunit arrangement of 5-HT_3 receptors. *Proc. Natl. Acad. Sci. USA.* 102:12595–12600.
20. Lochner, M., and S. C. Lummis. 2010. Agonists and antagonists bind to an A-A interface in the heteromeric 5-HT_3AB receptor. *Biophys. J.* 98:1494–1502.
21. Thompson, A. J., K. L. Price, and S. C. Lummis. 2011. Cysteine modification reveals which subunits form the ligand binding site in human heteromeric 5-HT_3AB receptors. *J. Physiol.* 589:4243–4257.
22. Price, K. L., and S. C. Lummis. 2005. FlexStation examination of 5-HT_3 receptor function using Ca^{2+}- and membrane potential-sensitive dyes: advantages and potential problems. *J. Neurosci. Methods.* 149:172–177.
23. Perez, J. B., K. L. Martinez, …, H. Vogel. 2006. Supported cell-membrane sheets for functional fluorescence imaging of membrane proteins. *Adv. Funct. Mater.* 16:306–312.
24. Son, C. D., F. J. Moss, …, H. A. Lester. 2009. Nicotine normalizes intracellular subunit stoichiometry of nicotinic receptors carrying mutations linked to autosomal dominant nocturnal frontal lobe epilepsy. *Mol. Pharmacol.* 75:1137–1148.
25. Nashmi, R., M. E. Dickinson, …, H. A. Lester. 2003. Assembly of $\alpha4\beta2$ nicotinic acetylcholine receptors assessed with functional fluorescently labeled subunits: effects of localization, trafficking, and nicotine-induced upregulation in clonal mammalian cells and in cultured midbrain neurons. *J. Neurosci.* 23:11554–11567.
26. Zheng, J., and W. N. Zagotta. 2004. Stoichiometry and assembly of olfactory cyclic nucleotide-gated channels. *Neuron.* 42:411–421.
27. Staruschenko, A., E. Adams, …, J. D. Stockand. 2005. Epithelial Na^+ channel subunit stoichiometry. *Biophys. J.* 88:3966–3975.
28. Grasser, E., B. Steinecker, …, W. Schreibmayer. 2008. Subunit stoichiometry of heterologously expressed G-protein activated inwardly rectifying potassium channels analyzed by fluorescence intensity ratio measurement. *Pflugers Arch.* 455:1017–1024.
29. Massoura, A. N., T. J. Dover, …, N. M. Barnes. 2011. The identification of N-glycosylated residues of the human 5-HT_3B receptor subunit: importance for cell membrane expression. *J. Neurochem.* 116:975–983.
30. Srinivasan, R., C. I. Richards, …, H. A. Lester. 2012. Förster resonance energy transfer (FRET) correlates of altered subunit stoichiometry in Cys-loop receptors, exemplified by nicotinic $\alpha4\beta2$. *Int. J. Mol. Sci.* 13:10022–10040.
31. Srinivasan, R., R. Pantoja, …, H. A. Lester. 2011. Nicotine up-regulates $\alpha4\beta2$ nicotinic receptors and ER exit sites via stoichiometry-dependent chaperoning. *J. Gen. Physiol.* 137:59–79.
32. Krzywkowski, K., P. A. Davies, …, A. A. Jensen. 2008. High-frequency HTR3B variant associated with major depression dramatically augments the signaling of the human 5-HT_3AB receptor. *Proc. Natl. Acad. Sci. USA.* 105:722–727.

33. Hammer, C., S. Cichon, …, B. Niesler. 2012. Replication of functional serotonin receptor type 3A and B variants in bipolar affective disorder: a European multicenter study. *Transcult. Psychiatry.* 2:e103.

34. Walstab, J., C. Hammer, …, B. Niesler. 2008. Naturally occurring variants in the HTR3B gene significantly alter properties of human heteromeric 5-hydroxytryptamine-3A/B receptors. *Pharmacogenet. Genomics.* 18:793–802.

35. Boyd, G. W., P. Low, …, C. N. Connolly. 2002. Assembly and cell surface expression of homomeric and heteromeric 5-HT_3 receptors: the role of oligomerization and chaperone proteins. *Mol. Cell. Neurosci.* 21:38–50.

36. Ilegems, E., H. M. Pick, …, H. Vogel. 2004. Noninvasive imaging of 5-HT_3 receptor trafficking in live cells: from biosynthesis to endocytosis. *J. Biol. Chem.* 279:53346–53352.

37. Drenan, R. M., R. Nashmi, …, H. A. Lester. 2008. Subcellular trafficking, pentameric assembly, and subunit stoichiometry of neuronal nicotinic acetylcholine receptors containing fluorescently labeled α6 and β3 subunits. *Mol. Pharmacol.* 73:27–41.

38. Boulin, T., M. Gielen, …, J. L. Bessereau. 2008. Eight genes are required for functional reconstitution of the *Caenorhabditis elegans* levamisole-sensitive acetylcholine receptor. *Proc. Natl. Acad. Sci. USA.* 105:18590–18595.